JOURNAL OF GEOPHYSICAL RESEARCH, VOL. 105, NO. D7, PAGES 9321-9333, APRIL 16, 2000

Influence of convection and biomass burning outflow on tropospheric chemistry over the tropical Pacific

Yuhang Wang,[1] Shaw C. Liu, Hongbin Yu, and Scott T. Sandholm
School of Earth and Atmospheric Sciences, Georgia Institute of Technology, Atlanta

Tai-Yih Chen and Donald R. Blake
Department of Chemistry, University of California, Irvine

Abstract. Observations over the tropics from the Pacific Exploratory Mission-Tropics A Experiment are analyzed using a one-dimensional model with an explicit formulation for convective transport. Adopting tropical convective mass fluxes from a general circulation model (GCM) yields a large discrepancy between observed and simulated CH_3I concentrations. Observations of CH_3I imply the convective mass outflux to be more evenly distributed with altitude over the tropical ocean than suggested by the GCM. We find that using a uniform convective turnover lifetime of 20 days in the upper and middle troposphere enables the model to reproduce CH_3I observations. The model reproduces observed concentrations of H_2O_2 and CH_3OOH. Convective transport of CH_3OOH from the lower troposphere is estimated to account for 40-80% of CH_3OOH concentrations in the upper troposphere. Photolysis of CH_3OOH transported by convection more than doubles the primary HO_x source and increases OH concentrations and O_3 production by 10-50% and 0.4 ppbv d^{-1}, respectively, above 11 km. Its effect on the OH concentration and O_3 production integrated over the tropospheric column is, however, small. The effects of pollutant import from biomass burning regions are much more dominant. Using C_2H_2 as a tracer, we estimate that biomass burning outflow enhances O_3 concentrations, O_3 production, and concentrations of NO_x and OH by 60%, 45%, 75%, and 7%, respectively. The model overestimates HNO_3 concentrations by about a factor of 2 above 4 km for the upper one-third quantile of C_2H_2 data while it generally reproduces HNO_3 concentrations for the lower and middle one-third quantiles of C_2H_2 data.

1. Introduction

Convection is a dominant process for the vertical distribution of chemical species in the troposphere. This distribution process, unlike diffusion, is strongly direction oriented. Updrafts bring up air from the lower troposphere into the free troposphere, and compensating subsidence takes free tropospheric air back down into the lower troposphere. Over industrialized continents, convection leads to efficient export of pollutants into the free troposphere and greatly enhances photochemistry outside the polluted continental lower troposphere [*Gidel*, 1983; *Chatfield and Crutzen*, 1984; *Dickerson et al.*, 1987; *Pickering et al.*, 1988, 1992; *Jaeglé et al.*, 1998].

Over tropical continents, convection exports large amounts of pollutants from biomass burning [*Crutzen and Andreae*, 1990]. *Fishman et al.* [1990] showed widespread high tropospheric O_3 columns over the tropical South Atlantic and adjacent continents during the biomass burning season (September-November). Estimated tropospheric O_3 column in the region is a factor of 2 higher than over the tropical Pacific. During the Transport and Atmospheric Chemistry Near the Equatorial Atlantic (TRACE A) Experiment in September-October, 1992, elevated concentrations of O_3, NO_x ($NO+NO_2$), CO, and hydrocarbons from biomass burning emissions were observed at all altitudes [*Fishman et al.*, 1996]. Transport of these pollutants evidently influences chemistry in the remote tropical Pacific [*Jacob et al.*, 1996; *Schultz et al.*, 1999].

Recent works suggest that local convection in remote tropical regions also has a large impact on chemistry in the upper troposphere [*Prather and Jacob*, 1997; *Jaeglé et al.*, 1997; *Cohan et al.*, 1999]. This effect arises from the large gradient of chemical species between the lower and upper troposphere. Photochemistry driven by radical production from photolysis of O_3 and the subsequent reaction of O^1D+H_2O is active in the lower troposphere due in part to the abundance of H_2O. In the upper troposphere, photochemistry is considerably slower; radical sources, such as photolysis of acetone, become much more important than O^1D+H_2O [*Singh et al.*, 1995; *Arnold et al.*, 1997; *McKeen et al.*, 1997b; *Jaeglé et al.*, 1997; *Wennberg et al.*, 1998; *Müller and Brasseur*, 1999]. As a result, photochemically produced chemical species tend to have much higher concentrations in the lower than in the upper troposphere. *Prather and Jacob* [1997] noted the large vertical gradient of CH_3OOH in the tropics and suggested that convection of CH_3OOH is a dominant radical source in the tropical upper troposphere.

[1]Now at Department of Environmental Sciences, Rutgers University, New Brunswick, New Jersey.

Paper number 1999JD901127.
0148-0227/00/1999JD901127$09.00

It is, however, not clear to what extent the radical source from convected CH_3OOH affects O_3 and OH concentrations in the tropical troposphere and how this effect compares with that of biomass burning. Using a one-dimensional model, we analyze tropical DC-8 observations from the Pacific Exploratory Mission-Tropics A (PEM-Tropics A) Experiment in September-October, 1996 [*Hoell et al.*, 1999]. Previous photochemical analyses for PEM-Tropics A [e.g., *Schultz et al.*, 1999; *Cohan et al.*, 1999; *Crawford et al.*, 1999] have used point models, which cannot directly simulate the effect of convection. The vertical transport in our model, which includes an explicit treatment for convective transport, is constrained using the observations of CH_3I since the vertical distribution of CH_3I is a sensitive indicator for marine convection [*Davis et al.*, 1996b; *Cohan et al.*, 1999]. On the basis of observations of O_3, NO, CO, and hydrocarbons, we investigate if the model can simulate observed vertical profiles of other chemical species such as peroxides and use the model to compute the column budget of O_3. We will examine the effect of convection on chemistry. We will also use C_2H_2 as a tracer of outflow from biomass burning regions [*Blake et al.*, 1996, 1999; *Andreae et al.*, 1996] to examine the effect of this pollutant import and compare this effect with that of local convection.

2. Model Description

The model is based on the one-dimensional model by *Trainer et al.* [1987, 1991] and *McKeen et al.* [1997a]. We extend the vertical domain to 16 km, the altitude of the tropical tropopause. The vertical resolution of the model decreases from 10 m near the surface to 1 km at 12-km altitude, which is the flight ceiling of the DC-8 aircraft. The top two layers are equally spaced between 12 and 16 km. Chemical species with lifetimes longer than 10 min are transported vertically. The time step for transport and chemistry is 30 s. The model is run for 60 days to obtain a steady state solution.

The mass continuity equation for a one-dimensional model is

$$\frac{\partial n_i}{\partial z} = P_i + L_i + \frac{\partial \Phi_i}{\partial z} \quad , \tag{1}$$

where n_i is the concentration of species i, P_i is the chemical production rate, L_i is the loss rate by chemical reactions and in the lowest model layer by dry deposition, and Φ_i is the flux due to vertical transport. We consider two types of vertical transport, diffusion and convection. Diffusion, which is the only transport mechanism used by *Trainer et al.* [1987], represents mixing by random motion of air parcels. In contrast, convection represents direct transport of the lower tropospheric air into the free troposphere followed by compensating subsidence. The need for invoking convective transport in our model becomes apparent in the simulation of CH_3I in section 3. Including convective transport also allows us to explicitly simulate wet scavenging of soluble species in the model. Previous one-dimensional models usually invoke a pseudo first-order loss rate constant to account for wet scavenging of soluble species [e.g., *Logan et al.*, 1981].

The vertical flux Φ_i is the sum of diffusive and convective fluxes. The diffusive flux Φ_d is a function of the vertical gradient of the chemical species i and the eddy diffusion coefficient K_z,

$$\Phi_d = NK_z \frac{\partial (n_i/N)}{\partial z} \quad , \tag{2}$$

where N is the concentration of air. The value of K_z in the surface layer (lower than 80 m in altitude) is calculated from similarity theory [*Trainer et al.*, 1987]. The value of K_z above the surface layer will be specified. Convective mass fluxes in the model are from the Goddard Institute for Space Studies (GISS) general circulation model (GCM) (version II') as previously used by *Prather and Jacob* [1997]. We will discuss the model vertical transport constrained by CH_3I observations in section 3.

The chemical mechanisms in the model are updated from the compilations by *DeMore et al.* [1997] and *Atkinson et al.* [1997]. Quantum yields and cross sections for photolysis of acetone are from *Gierczak et al.* [1998]. The reaction rate constants of OH with HNO_3 and NO_2 are updated from *Brown et al.* [1999a, b]. The model does not include N_2O_5 hydrolysis on aerosols [*Schultz et al.*, 2000]. The total ozone column is specified to be 268 Dobson units (DU), the average measured for the tropical region during PEM-Tropics A by the Total Ozone Mapping Spectrometer. A surface albedo of 0.1 is specified for the ocean. We compared model computed photolysis rates of $J(O^1D)$ and $J(NO_2)$ with observations for solar zenith angle <50°, when the value of $J(NO_2)$ is largely invariable to solar zenith angle. The model averages agree to within ±12% with mean and median values of the observations binned in 1-km intervals. Dry deposition velocities to water are specified to be 1 cm s^{-1} for soluble species HNO_3 and H_2O_2 and less than 0.1 cm s^{-1} for other species [*Wang et al.*, 1998a].

3. Vertical Transport Constrained by CH_3I Observations

We use observed CH_3I concentrations to adjust the parameters of our vertical transport scheme. Methyl iodide is emitted largely from the ocean [*Andreae*, 1990; *Bates et al.*, 1992; *Happell and Wallace*, 1996]. It is lost primarily by photolysis. Its photochemical lifetime is about 3 days near the surface and 2 days in the upper troposphere. Its vertical distribution therefore depends critically on the vertical transport of CH_3I from the marine lower troposphere. Furthermore, the detection limit of CH_3I during PEM-Tropics A is low (0.01 parts per trillion by volume (pptv)) [*Cohan et al.*, 1999], making CH_3I observations a valuable constraint on the model transport scheme. *Blake et al.* [1996] estimated that CH_3I emissions from biomass burning during TRACE-A are much smaller than the oceanic source. The vertical profiles of CH_3I compiled for the lower, middle, and upper one-third quantiles of C_2H_2, a tracer for biomass burning, also do not exhibit enhancements of CH_3I associated with upper quantiles of C_2H_2, suggesting that observed CH_3I originates primarily from the ocean. We specified the CH_3I concentration at 500-m altitude in the model to the observed value.

Figure 1 shows simulated CH_3I concentrations using different vertical transport schemes. The two diffusion-only simulations show the largest discrepancies. For these simulations we specified the values of K_z as 10 and 60 m s^{-2} above the surface layer, respectively. For comparison, values of K_z in the troposphere derived from measurements of ^{222}Rn in the eastern United States vary from 40 m^2 s^{-1} in summer to 20 m^2 s^{-1} in

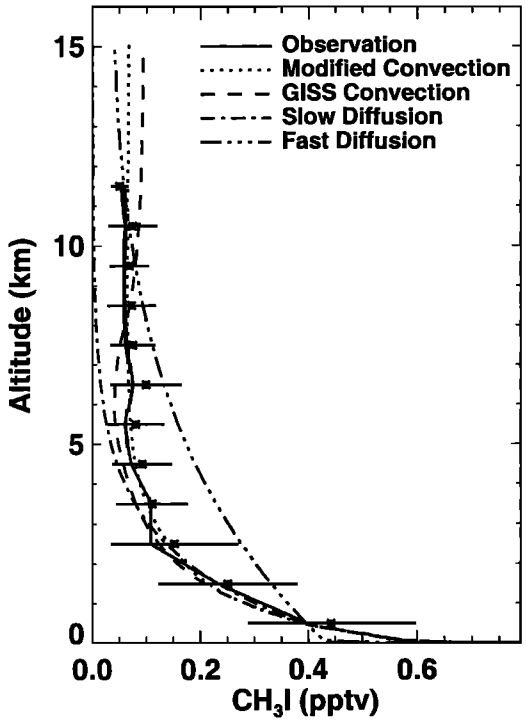

Figure 1. Comparison between observed and simulated vertical profiles of CH_3I concentrations. The observations over the tropical Pacific (20°S-20°N) are binned vertically in 1-km intervals. The solid line represents the median profile. Asterisks and horizontal bars are means and standard deviations, respectively, of the observations. Four model simulations using different vertical transport schemes are shown (see text for details). The concentration of CH_3I at 500 m is specified in the model as the observed median at 0-1 km.

spring and fall [*Liu et al.*, 1984]. In the slow diffusion case (K_z = 10 m s^{-2}) the simulation agrees well with the observations below 2 km but drastically underestimates CH_3I concentrations in the middle and upper troposphere. Adopting a faster diffusion coefficient (K_z = 60 m s^{-2}) elevates simulated CH_3I concentrations to observed values at 10-12 km but also leads to gross overestimates in the middle and lower troposphere. These large discrepancies reflect the dominance of tropical convective transport, which cannot be approximated by a diffusion scheme.

Table 1 shows the convective mass outflux over the equatorial region (12°S-12°N) from the GISS GCM, version II' [*Rind and Lerner*, 1996]. The statistics of nonentraining, deep convection have been used by *Prather and Jacob* [1997]. The convective mass outflux below 10 km is significantly larger in Table 1 than reported by *Prather and Jacob* [1997] due to the addition of entraining convection in the statistics. Figure 1 shows the simulation of CH_3I concentrations based on these convective statistics. The value of K_z is specified as 10 m s^{-2} above the surface layer to reproduce the observed CH_3I vertical gradient in the lower troposphere. This simulation is much closer to the observations compared with diffusion-only simulations. However, it overestimates CH_3I concentrations at 9-12 km but underestimates at 4-7 km, reflecting the "C"-shaped profile of the GISS convective statistics. Similar discrepancies were found in a global simulation of CH_3I driven by assimilated meteorological data from the Goddard Earth Observation System Data Assimilation System (M. Schultz, personal communication, 1999).

Observations of CH_3I in the tropics therefore argue for a more uniformly distributed profile of the convective mass outflux with altitude over the tropical ocean than suggested by the GISS model. *Smyth et al.* [1996] also found that mixing of CO and hydrocarbons from the continental boundary layer into the middle troposphere is as efficient as mixing into the upper troposphere in the tropical western Pacific. We redistributed the GISS convective outflux of deep convection (>3-km altitude) evenly by air density (Table 1). The difference in mass outflux above 3 km reflects the difference in air mass among different layers. The resulting CH_3I concentrations in the model agree well with observations (Figure 1). The redistributed convective mass outflux, which yields a uniform convective turnover lifetime of 20 days above 3 km, will be used in the model to examine the effect of convection on chemistry in the tropics (section 5). Our results cannot rule out the possibility of greater convective outflux above 12 km compared with lower altitudes as indicated by the GISS model, because observations of CH_3I are unavailable above 12 km during PEM-Tropics A.

4. Influence of Biomass Burning Outflow

Biomass burning took place in Australia, southern Africa, and South America during the PEM-Tropics A period [*Olson et al.*, 1999]. Its strong influence was reflected in the observations over the tropical Pacific [*Blake et al.*, 1999; *Schultz et al.*, 1999; *Talbot et al.*, 1999]. A good tracer of tropical biomass burning is C_2H_2 [*Blake et al.*, 1996, 1999; *Andreae et al.*, 1996]; almost all C_2H_2 data between 0° and 20°N were below 30 pptv, whereas observations in the southern tropics often exceeded this level. We group observations in the tropics (20°S-20°N) on the basis of concurrent measurements of C_2H_2 to analyze the effect of biomass burning.

Three vertical profiles of observed chemical species (binned in 1-km intervals) are compiled corresponding to the

Table 1. Convective Mass Outflux

Altitude Range, km	GISS Flux[a], g m^{-2} s^{-1}	Modified Flux[b], g m^{-2} s^{-1}
10-16	1.6	0.88
7.5-10	0.8	0.76
5-7.5	0	0.90
3-5	1.1	0.96
1.5-3	2.2	2.2
0.7-1.5	-3.1	-3.1
0-0.7	-2.6	-2.6

[a] Convective statistics over the equatorial region (12°S-12°N) in the GISS II' general circulation model between May and August (M. Prather, personal communication, 1999). Positive values are mass outfluxes of convection; negative values reflect convergence in the lower troposphere feeding the convection. The upward convective mass transport is compensated for by subsidence as required by mass balance.

[b] Redistributed uniformly above 3 km by air density to reproduce observed CH_3I concentrations (Figure 1).

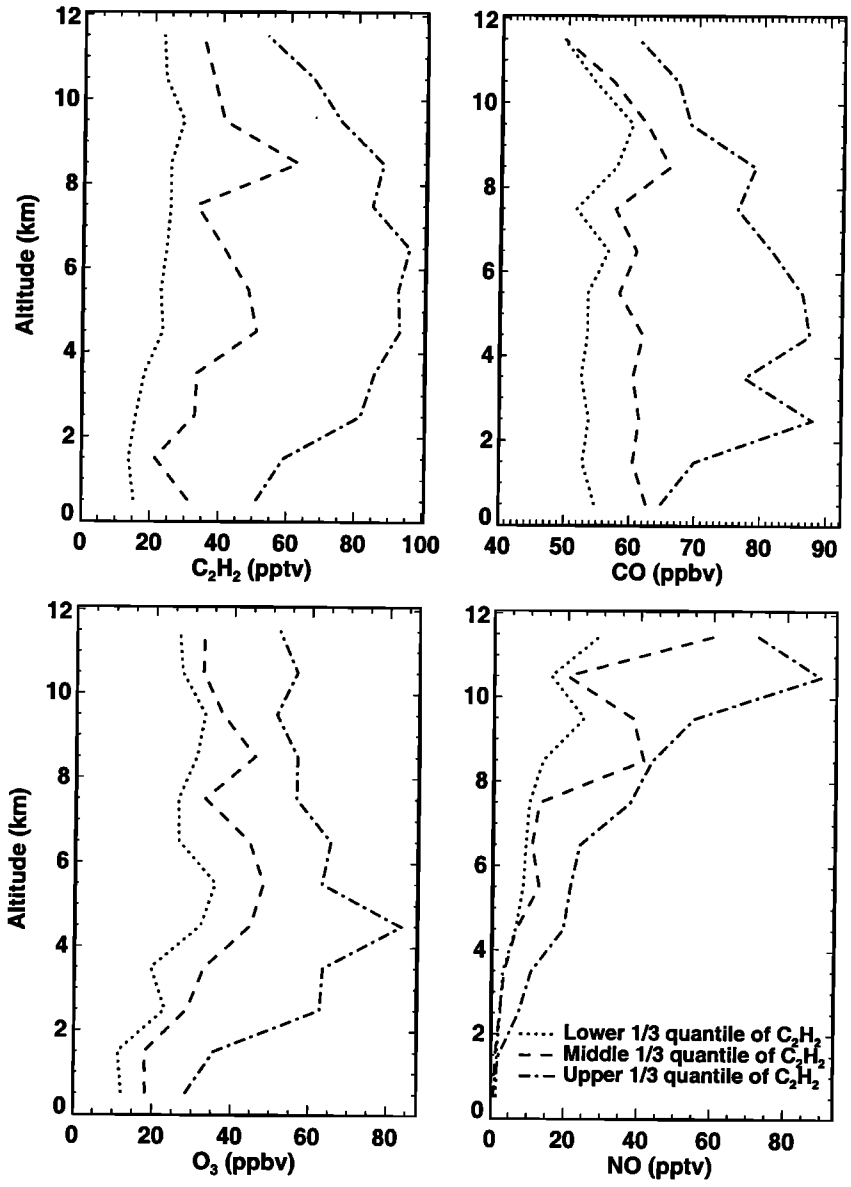

Figure 2. Observed median vertical profiles of C_2H_2, CO, O_3, and NO for three equally divided quantiles of C_2H_2 over the tropical Pacific. Observations are binned vertically in 1-km intervals.

lower, middle, and upper one-third quantiles of C_2H_2 concentrations. This simple grouping separates air masses significantly influenced by biomass burning outflow with high C_2H_2, CO, O_3, and NO concentrations from those with much lower concentrations (Figure 2). The median concentration of C_2H_2 increases from about 20 pptv in the lower one-third quantile to 60-80 pptv in the upper one-third quantile. The chemical lifetime of C_2H_2 against OH oxidation is only 1-2 weeks in the tropics. The factor of 3-4 enhancement of C_2H_2 concentrations from the lower to the upper one-third quantile therefore indicates strong influence of biomass burning outflow in the region. Another biomass burning tracer, CO, shows an increase of 20-80% from the lower to the upper one-third quantile of C_2H_2. This increase is smaller because of background CO concentrations from CH_4 oxidation [e.g., *Logan et al.*, 1981]. The small CO vertical gradient is due to its much longer lifetime (about 1 month in the lower troposphere and over 2 months in the upper troposphere) relative to convective turnover, which we estimate to be about 20 days (section 3). If CH_4 oxidation were its sole source, the CO concentration would be about 40 ppbv in the tropics. The enhancement of CO over a background of 40 ppbv shows large increases from the lower to the upper one-third quantile of C_2H_2, which is consistent with the enhancement of C_2H_2. Biomass burning also emits large amounts of NO that can lead to enhanced O_3 concentrations from the increasing in situ production [e.g., *Crutzen and Andreae*, 1990]. Concentrations of NO in biomass burning outflow may be further enhanced by lightning production [e.g., *Wang et al.*, 1998b]. Observed concentrations of O_3 and NO concentrations show corresponding increases with C_2H_2 (Figure 2). Column O_3 and NO_x concentrations (0-12 km) for different quantiles of C_2H_2 are listed in Table 2.

Table 2. Column O_3 Budget and OH and NO_x Concentrations

One-Third Quantile of C_2H_2	O_3[a]	$P(O_3)$[a]	$L(O_3)$[a]	OH[b]	NO_x[c]
Lower	14	1.4	3.7	1.4	2.0
Middle	20	1.7	4.5	1.5	3.1
Upper	34	3.1	5.5	1.6	5.4

Integrated over the air column of 0-12 km (20°S-20°N). Model values are 24-hour averages.

[a]Model-computed chemical production of O_3 from reactions of NO and peroxy radicals and loss from the reaction of O^1D+H_2O and reactions of O_3 with OH and HO_2 [*Davis et al.*, 1996a]. Column ozone is in Dobson units. Column production ($P(O_3)$) and loss ($L(O_3)$) of O_3 are in 10^{11} molecules cm^{-2} s^{-1}.

[b]Mass weighted column mean OH concentrations (in 10^6 molecules cm^{-3}) computed using the one-dimensional model.

[c]Concentrations of NO_x are computed using the one-dimensional model constrained to match observed daytime NO concentrations shown in Figure 2. Column NO_x is in 10^{14} molecules cm^{-2}.

5. Model Simulations: Effects of Convection and Biomass Burning Outflow

We constrain the one-dimensional model by observed median concentrations of O_3, NO, CO, nonmethane hydrocarbons (NMHCs), and H_2O for the lower, middle, and upper one-third quantiles of C_2H_2. Concentrations of NO_x are constrained in the model such that simulated daytime mean NO concentrations match the observed NO profiles. Among NMHCs, only long-lived C_2H_6, C_3H_8, and C_2H_2 were observed in significant amounts [*Blake et al.*, 1999]. Acetone was not measured during PEM-Tropics A. Observations during the Pacific Exploratory Mission (PEM-West B) show acetone concentrations above 200 pptv and below 400 pptv in the tropics [*Singh et al.*, 1995]. We therefore specify acetone concentrations of 200 and 400 pptv for data groups of the lower and upper one-third quantiles of C_2H_2, respectively. We specify for the middle one-third quantile of C_2H_2 a concentration of 300 pptv based on a global three-dimensional model simulation by *Wang et al.* [1998a, b]. The concentration of CH_4 is specified at 1.7 ppmv. The DC-8 flight ceiling was at about 12 km; we assume constant mixing ratios above 12 km to be the observed medians at 11-12 km for most species except for water vapor, which decreases with altitude to 6 ppmv at the tropopause.

5.1. Hydrogen Oxides

Concentrations of OH or HO_2 radicals were not measured on the DC-8 during PEM-Tropics A. We evaluate the model simulations using observations of the reservoirs of these radicals, H_2O_2 and CH_3OOH. In situ chemistry generally plays a central role in determining peroxide concentrations since their lifetimes in the tropics are less than 1 day in the lower troposphere and about 2 days in the upper troposphere. An exception is in the upper troposphere, where convective transport can greatly change their concentrations. In section 3 we have estimated a convective turnover lifetime of 20 days for the ventilation of the upper troposphere. Although this timescale is considerably longer than the lifetimes of peroxides, the peroxide concentrations are about a factor of 10 higher in the lower than in the upper troposphere (Figure 3). As a result, convective transport of air masses from the lower troposphere may provide a source of peroxides similar to in situ production. This effect does not apply to H_2O_2 since H_2O_2 is soluble, whereas the solubility of CH_3OOH is very low [*Lind and Kok*, 1986]. *Cohan et al.* [1999] estimated that 50-70% of convected H_2O_2 is scavenged, suggesting that convection has a small impact on upper tropospheric H_2O_2 concentrations.

Figure 3 compares observed and simulated H_2O_2 concentrations. We conducted simulations with wet scavenging coefficients of 50% and 100% for H_2O_2. A 100% scavenging coefficient corresponds to a complete removal of H_2O_2 from the convective air masses. The lower H_2O_2 concentrations simulated with a scavenging coefficient of 100% are in closer agreement with observations in the upper troposphere. The difference between the two simulations is small in the lower and middle troposphere. Thus we select the scavenging coefficient of 100% in our standard model.

Hydrogen peroxide is produced by the self-reaction of HO_2 and chemically destroyed by photolysis and the reaction with OH. The HO_2 self-reaction is the dominant pathway for HO_x (OH + peroxy radicals) loss under low NO_x conditions in the lower troposphere [*Kleinman*, 1994]. The HO_x loss is balanced by the HO_x production, which is largely photolysis of O_3 followed by the reaction of O^1D+H_2O in the lower and middle troposphere [*Logan et al.*, 1981]. Although O_3 concentrations increase by a factor of 2 from the lower to the upper one-third quantile of C_2H_2 (Figure 2), air masses with high C_2H_2 concentrations were much drier (Figure 4). The relative humidity for the lower one-third quantile C_2H_2 decreases from 80% in the lower troposphere to 15% in the upper troposphere. It is 50-300% higher than that for the upper one-third quantile of C_2H_2. The compensating effects of O_3 and H_2O on the source of HO_x are reflected in comparable H_2O_2 concentrations for the three quantiles of C_2H_2 simulated in the model.

Observed H_2O_2 concentrations are similar for the lower and middle one-third quantiles of C_2H_2 but are lower for the upper one-third quantile of C_2H_2. The lower H_2O_2 concentrations (in the lower and middle troposphere) are not reproduced by the model. Comparison of observed and simulated CH_3OOH concentrations (Figure 3) shows a more pronounced overestimate for the upper one-third quantile of C_2H_2. The CH_3OOH budget for 0°-30°S by *Schultz et al.* [1999] also shows larger chemical production of CH_3OOH than loss in the lower and middle troposphere. A possible explanation is that dry, high C_2H_2 concentration air masses, which originated most likely from the continents, have not reached chemical steady state with respect to peroxides and hence have lower peroxide concentrations.

Convective transport largely enhances CH_3OOH concentrations in the upper troposphere (Figure 3), as suggested by *Prather and Jacob* [1997]. Model results with convective

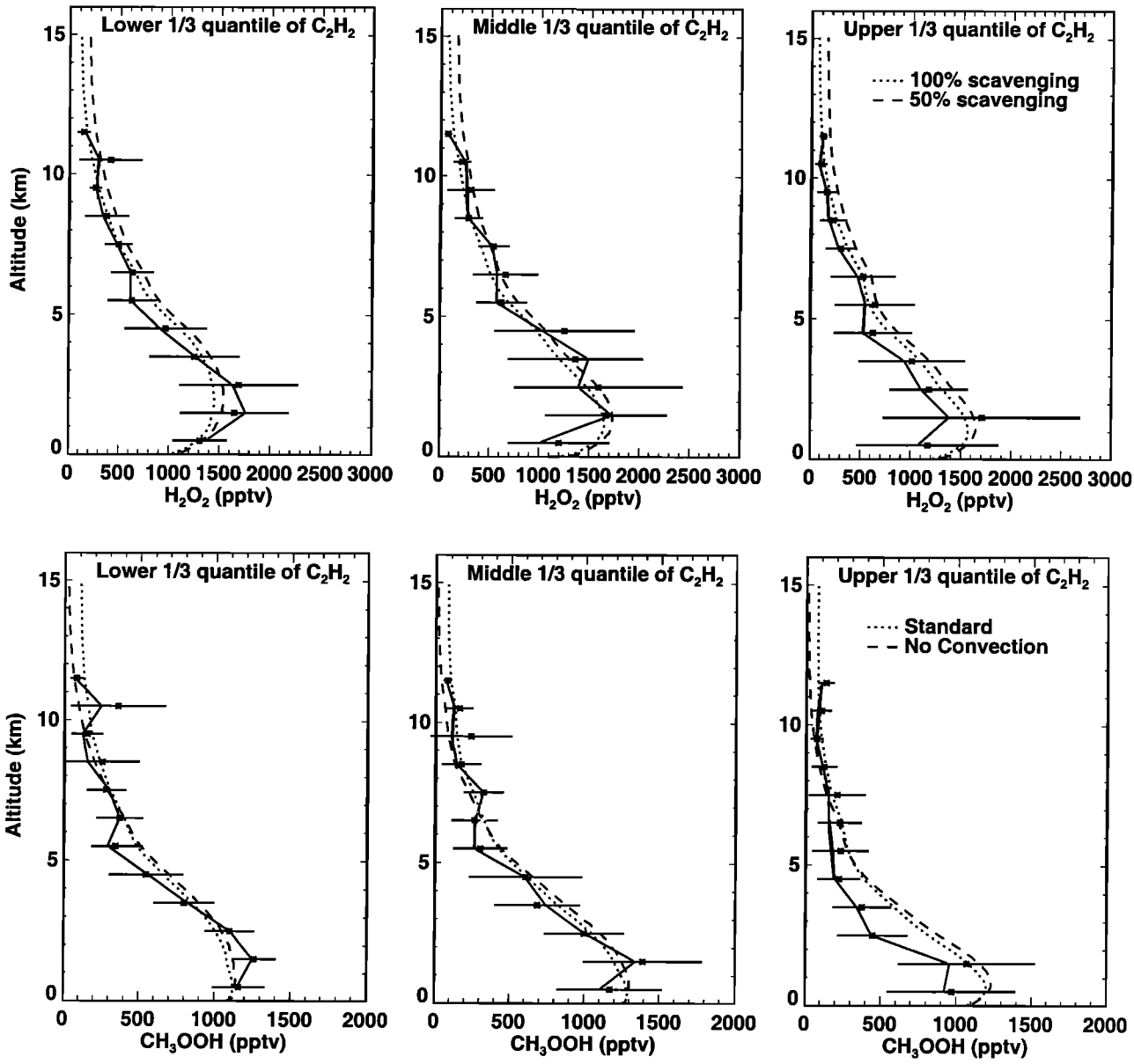

Figure 3. Comparison of observed and simulated vertical profiles of H_2O_2 and CH_3OOH for the lower, middle, and upper one-third quantiles of C_2H_2. Symbols for the observations are the same as in Figure 1. Model simulations of H_2O_2 concentrations are shown with scavenging coefficients of 100% and 50%. Model simulations of CH_3OOH concentrations are shown with and without convective transport.

transport agree better with the observations above 10 km than without convection. Figure 5 shows the fraction of CH_3OOH attributed to convective transport in our standard model. The fraction is large in the upper troposphere, increasing from 40% at 10 km up to 80% at 15 km. Below 6 km the fraction drops to less than 20%. In this region the increase of CH_3OOH from convective transport is not enough to offset the decrease due to subsidence of air with lower CH_3OOH concentrations, resulting in lower CH_3OOH concentrations compared with the simulation without convection (Figure 3).

Photolysis of CH_3OOH convected from the lower troposphere provides a significant primary HO_x source that drives chemistry faster in the upper troposphere. Figure 6 compares primary HO_x sources, O^1D+H_2O, photolysis of acetone, and photolysis of CH_3OOH and CH_2O transported from the lower troposphere by convection (for the middle one-third quantile of C_2H_2). Photolysis of O_3 followed by the reaction of O^1D+H_2O dominates the primary HO_x sources up to 10 km. The rapid decrease of this source with altitude reflects decreasing H_2O levels (Figure 4). The HO_x sources from photolysis of acetone and convected CH_3OOH are less variable with altitude and surpass that from O^1D+H_2O above 11 km. Convective transport of CH_3OOH more than doubles the total primary source of HO_x in the upper troposphere. The source from photolysis of convected CH_2O is a factor of 5-10 smaller than that from convected CH_3OOH.

The total HO_x production is larger than the sum of its primary sources because of photolysis of H_2O_2 and CH_3OOH

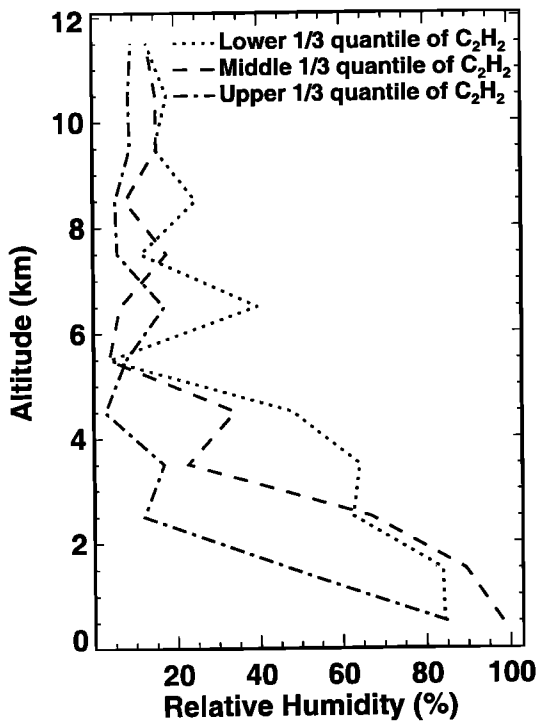

Figure 4. Same as Figure 2 but for relative humidity (over water). Water vapor concentrations measured by the differential absorption CO measurement (DACOM) instrument are used.

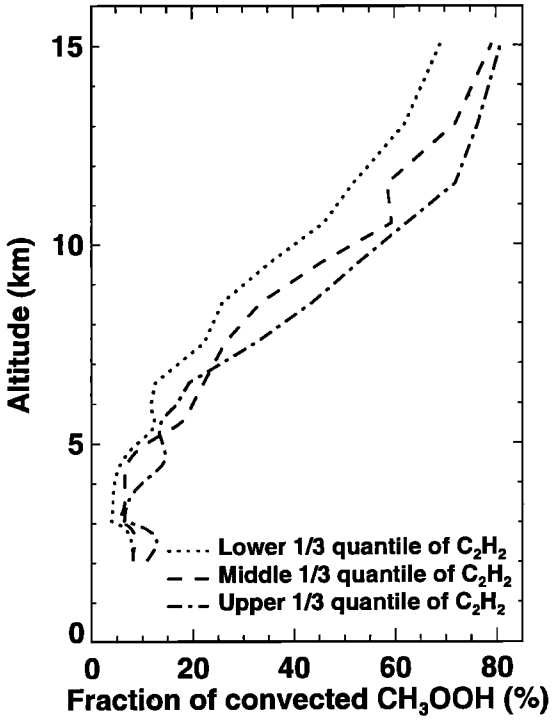

Figure 5. Fraction of CH_3OOH attributed to convective transport as a function of altitude for the lower, middle, and upper one-third quantiles of C_2H_2.

produced in situ and photolysis of CH_2O from CH_4 oxidation. Figure 7 compares the total HO_x production with and without convection. The increase of total HO_x production due to convective transport of CH_3OOH is apparent above 10 km by up to a factor of 3. Below 8 km, HO_x production with convection tends to be lower than without convection due to lower H_2O_2 and CH_3OOH concentrations in the convective case (Figure 3). The concentration of OH shows corresponding changes but with smaller magnitudes (Figure 7); the maximum increase is less than 50% in the upper troposphere. The increase of HO_x production due to convection of CH_3OOH has a negligible effect on the column mean OH concentration.

5.2. Ozone

The additional HO_x source from CH_3OOH transported by convection enhances in situ O_3 production in the upper troposphere [*Prather and Jacob*, 1997; *Jaeglé et al.*, 1997]. Figure 8 compares the O_3 production rate between simulations with and without convection for the middle one-third quantile of C_2H_2. Ozone is produced by reactions of NO and peroxy radicals. The production rate increases by about 0.4 ppbv d^{-1} above 11 km. Integrated over the tropospheric column (0-16 km), the production rate of O_3 increases by only 4% from 1.88×10^{11} to 1.96×10^{11} molecules cm^{-2} s^{-1}.

The effect of biomass burning outflow is much larger in comparison. Observed ozone columns of 0-12 km are 14, 20, and 34 DU for the lower, middle, and upper one-third quantiles, respectively, of C_2H_2 (Table 2). Assuming the lower one-third quantile of C_2H_2 data are not significantly influenced by outflow from biomass burning regions, we estimate an increase of 60% or 9 DU due to enhanced O_3 concentrations in

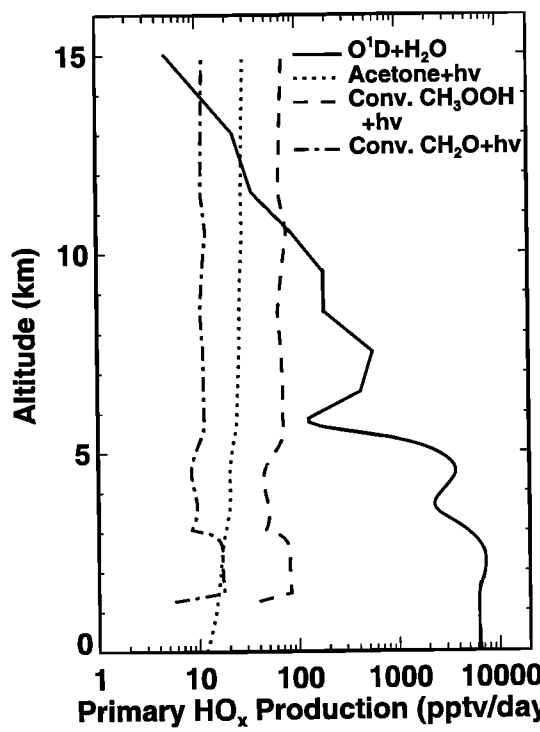

Figure 6. Simulated primary sources of HO_x, O^1D+H_2O, photolysis of acetone, and photolysis of CH_3OOH and CH_2O transported from the lower troposphere by convection, as a function of altitude for the middle one-third quantile of C_2H_2. The HO_x yield of CH_2O photolysis is computed on line.

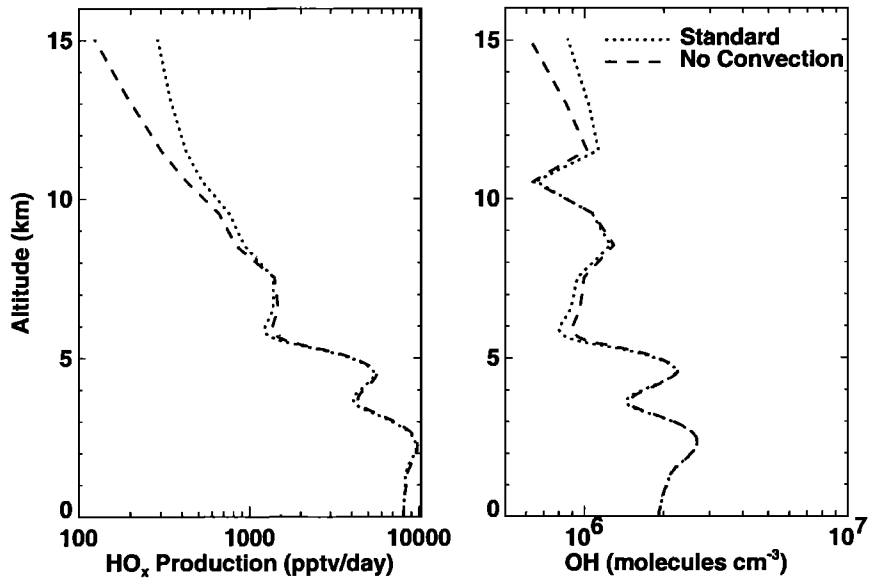

Figure 7. Simulated total HO_x production and OH concentrations as a function of altitude for the middle one-third quantile of C_2H_2 with and without convection.

biomass burning outflow. The column mean OH concentrations are $1.4x10^6$, $1.5x10^6$, and $1.6x10^6$ molecules cm^{-3} for the lower, middle, and upper one-third quantiles, respectively, of C_2H_2, corresponding to a relatively small enhancement of 7% due to biomass burning outflow. The small increase in the OH concentration reflects in part the compensating effects of concurrent increases of NO_x and CO concentrations with C_2H_2; NO_x tends to increase OH concentrations, while CO has the opposite effect.

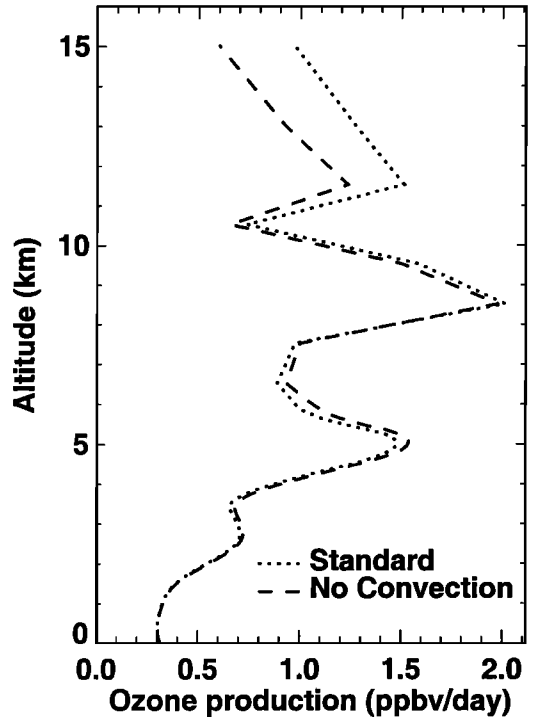

Figure 8. Same as Figure 7 but for the O_3 production rate.

Figure 9 shows simulated production and loss rate and the chemical lifetime of O_3 for the middle one-third quantile of C_2H_2. The production rate of O_3 increases slightly with altitude and is more uniformly distributed vertically than the loss rate. The loss of O_3 occurs primarily in the lowest 5 km. Integrated over the air column of 0-12 km, about 70% of O_3 loss occurs at 0-3 km and 20% occurs at 4-5 km. The column O_3 production (0-12 km) is $1.7x10^{11}$ molecules cm^{-2} s^{-1}, less than half of the column O_3 loss of $4.5x10^{11}$ molecules cm^{-2} s^{-1} (Table 2). About 70% of the O_3 loss is due to the reaction of O^1D+H_2O. The remaining fraction is due to O_3 reactions with OH and HO_2. The chemical lifetime of O_3 increases from 4.5 days near the surface to over 300 days at 15 km.

Air masses with higher concentrations of C_2H_2 have higher concentrations of NO (Figure 2), which is produced most likely from biomass burning and lightning during convection. Higher NO concentrations tend to increase in situ production of O_3. The column O_3 production of 0-12 km are $1.4x10^{11}$, $1.7x10^{11}$, and $3.0x10^{11}$ molecules cm^{-2} s^{-1} for the lower, middle, and upper one-third quantiles, respectively, of C_2H_2 (Table 2). Assuming as previously that the lower one-third quantile of C_2H_2 data represent air masses not significantly influenced by outflow from biomass burning regions, we estimate that the column production of O_3 is increased by 45%, or $6.3x10^{10}$ molecules cm^{-2} s^{-1}, due to biomass burning outflow.

Our estimate of the column O_3 production of $1.7x10^{11}$ molecules cm^{-2} s^{-1} compares well with $2.0x10^{11}$ molecules cm^{-2} s^{-1} over the tropical North Pacific calculated by *Davis et al.* [1996a] and $1.4\text{-}1.8x10^{11}$ molecules cm^{-2} s^{-1} over the tropical South Pacific calculated by *Schultz et al.* [1999]. Our estimated column O_3 loss of $4.5x10^{11}$ molecules cm^{-2} s^{-1} is, however, significantly higher than $2.9x10^{11}$ molecules cm^{-2} s^{-1} calculated by *Davis et al.* [1996a] and $3.2x10^{11}$ molecules cm^{-2} s^{-1} calculated by *Schultz et al.* [1999]. Compared with median values compiled by *Davis et al.* [1996a] (for PEM-West A), median O_3 and H_2O concentrations for the middle one-third quantile of C_2H_2 used in our model during PEM-

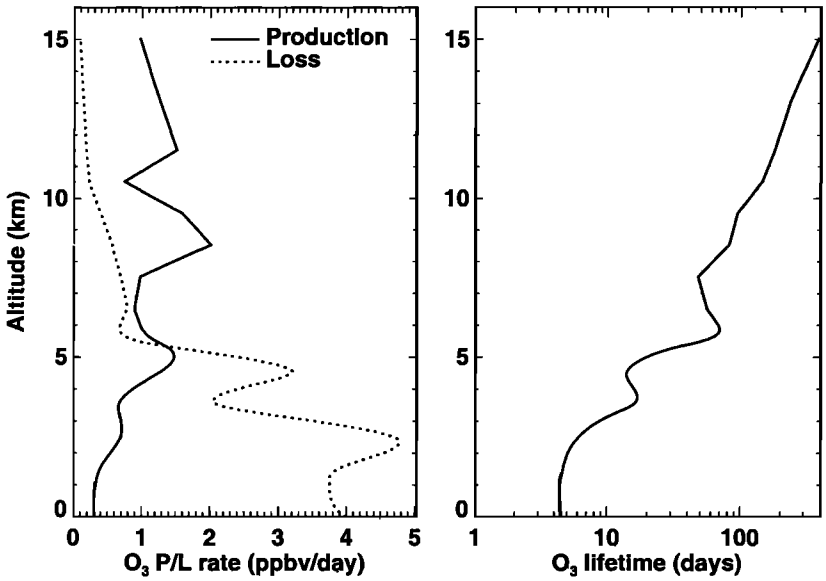

Figure 9. Simulated O_3 production and loss rate and its chemical lifetime as a function of altitude for the middle one-third quantile of C_2H_2.

Tropics A (Figure 2) are both up to a factor of 2 greater at 0-4 km. The difference between our estimate and that of *Schultz et al.* [1999] largely reflects the difference in the data selection method and the large variability in observed H_2O concentrations. Data shown in Figure 9 correspond to median concentrations for the middle one-third quantile of C_2H_2. Median concentrations of O_3 and H_2O selected in this manner tend to be higher than the median concentrations for all the data. The difference is much larger for H_2O than O_3. For instance, median H_2O concentrations are factors of 2 and 6 higher at 2-3 and 4-5 km, respectively, for the middle one-third quantile of C_2H_2 than for all the data. High H_2O concentrations at these altitudes are reflected in the O_3 loss rate in Figure 9. The uncertainty in the model estimate of the column O_3 loss tends to be larger than that of the column O_3 production since the former estimate relies largely on a subset of observations (below 3 km) that also have large variability.

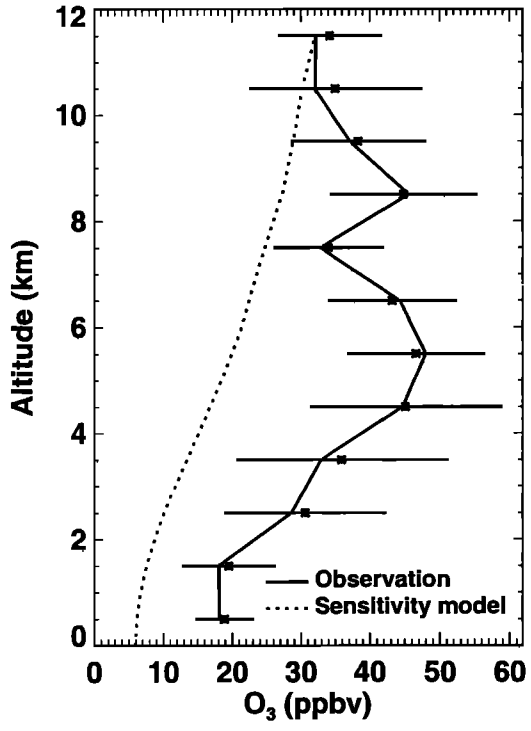

Figure 10. Comparison of observed and simulated vertical profiles O_3 for the middle one-third quantile of C_2H_2. Symbols are the same as in Figure 1. The concentration of O_3 at 11-12 km is specified as observed in the sensitivity simulation.

The net column O_3 deficits (0-12 km) computed in our model are 2.3×10^{11}, 2.8×10^{11}, and 2.4×10^{11} molecules cm^{-2} s^{-1} for the lower, middle, and upper one-third quantiles, respectively, of C_2H_2. The largest deficit is for the middle one-third quantile of C_2H_2 due to a combination of high relative humidity and relatively high O_3 concentrations (Figures 2 and 4). *Schultz et al.* [1999] suggested that the large O_3 deficit is supplied mostly by longitudinal transport of O_3 into the region. We conduct a sensitivity simulation; the concentration of O_3 at 11-12 km is specified as observed, below which altitude O_3 concentrations are determined by chemical production and loss and a downward flux of O_3 from the upper troposphere due to subsidence. The resulting O_3 concentrations are much lower than the observations (Figure 10). The O_3 column of 0-12 km in the sensitivity simulation is 50% lower, suggesting large amounts of lateral import of O_3 in the region, in agreement with *Schultz et al.* [1999].

5.3. Nitrogen Oxides

Simulated HNO_3 concentrations are generally within the range of observations for the lower and middle one-third quantiles of C_2H_2 but are about a factor of 2 higher above 4 km for the upper one-third quantile of C_2H_2 (Figure 11). Using rate constants for reactions of OH with NO_2 and HNO_3 from *Brown et al.* [1999a, b], instead of those recommended by *Demore et al.* [1997], decreases HNO_3 concentrations by 5-20

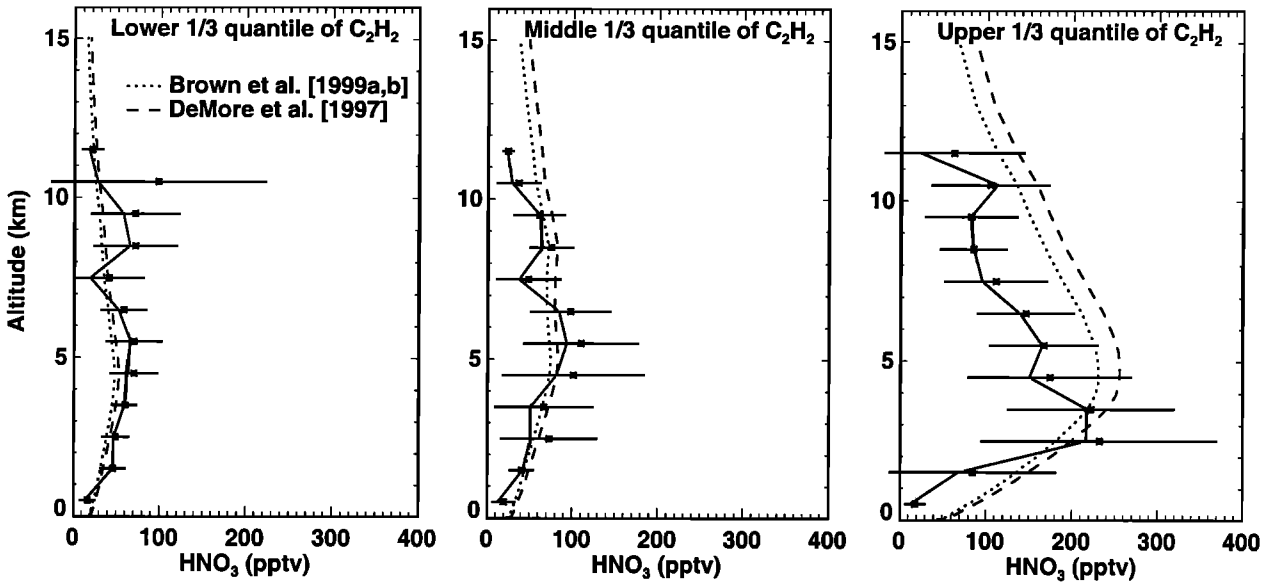

Figure 11. Same as Figure 3 but for HNO_3. Model simulations are shown for using reaction rate constants of OH with NO_2 and HNO_3 from *Brown et al.* [1999a, b] and *DeMore et al.* [1997].

pptv. The relative reduction of HNO_3 concentrations increases with altitude to 20-30% in the upper troposphere. However, only in the case of the upper one-third quantile of C_2H_2 is the agreement between model and observations markedly improved when using the new rate constants.

Model simulations of HNO_3 in the troposphere generally overestimate observations by more than a factor of 2 on a global scale [e.g., *Wang et al.*, 1998b; *Lawrence and Crutzen*, 1998; *Hauglustaine et al.*, 1998]. A number of hypotheses have been proposed to explain this discrepancy [e.g., *Schultz et al.*, 2000]. As in other models, ours does not resolve fractionation of HNO_3 into the aerosol phase. However, *Schultz et al.* [2000] found that aerosol nitrate concentrations were very low during PEM-Tropics A. The hypothesis that rapid chemical recycling of HNO_3 to NO_x in sulfate aerosols or on soot [*Chatfield*, 1994; *Fan et al.*, 1994; *Hauglustaine et al.*, 1996; *Jacob et al.*, 1996; *Lary et al.*, 1997] is compatible with our results because both sulfur and soot are emitted from biomass burning. *Wang et al.* [1998b] found some evidence for the chemical recycling in biomass burning outflow over the tropical South Atlantic during TRACE-A. Loss of HNO_3 due to deposition to cirrus ice crystals followed by subsequent removal by gravitational settling [*Lawrence and Crutzen*, 1998] cannot explain the dependence of HNO_3 overestimates on high C_2H_2 concentrations and appears to be inconsistent with our results. Another explanation for our results could be that air masses with high C_2H_2 concentrations are recently exported from biomass burning regions and have not reached chemical steady state with respect to HNO_3.

Observed peroxyacetylnitrate (PAN) concentrations above 4 km increase from 20 pptv in the lower one-third quantile of C_2H_2 to about 100 pptv in the upper one-third quantile of C_2H_2 (Figure 12). Concentrations of PAN are much lower below 4 km due in part to its short lifetime (20 min to 1 day) against thermolysis. The rate constant of thermolysis decreases exponentially with decreasing temperature and becomes insignificant above 7 km in comparison with photolysis [*Talukdar et al.*, 1995]. The chemical lifetime of PAN in the upper troposphere, controlled by photolysis, is much longer (about 1 month). Model results compare reasonably well with observations for the lower one-third quantile of C_2H_2 but tend to be much lower (up to 40 pptv) for the middle and upper one-third quantile of C_2H_2. The model underestimates likely reflect the influx of relatively long-lived PAN similar to the influxes of O_3 (section 5.2) and C_2H_2 (section 4) associated biomass burning outflow. *Schultz et al.* [1999] suggested that PAN transported from biomass burning regions provides the major source of NO_x in the lower troposphere.

6. Conclusions

We applied a one-dimensional model with an explicit formulation for convective transport to analyze observations over the tropical Pacific during PEM-Tropics A. The vertical transport of the model is constrained by the observations of CH_3I, which originates primarily from the ocean and has a short lifetime of 2-3 days in the tropics. Observed CH_3I concentrations decrease rapidly with altitude in the lowest 3 km but show little dependence on altitude above 5 km. Using diffusive transport alone in the model cannot reproduce the observed profile. When tropical convective mass fluxes from a GCM (GISS model II') are applied, the model grossly overestimates CH_3I concentrations in the upper troposphere but largely underestimates CH_3I in the middle troposphere, indicating that convective mass outflux over the tropical ocean is more evenly distributed with altitude than suggested by the GISS statistics. In order to match observed CH_3I concentrations, the GISS convective outflux above 3 km is redistributed evenly (by air density), yielding a uniform convective turnover lifetime of 20 days. Observations of CH_3I above 12 km, not available during PEM-Tropics A, are necessary to constrain the convective turnover lifetime there.

The model generally reproduces observations of H_2O_2 and CH_3OOH. We find that efficient convective scavenging of

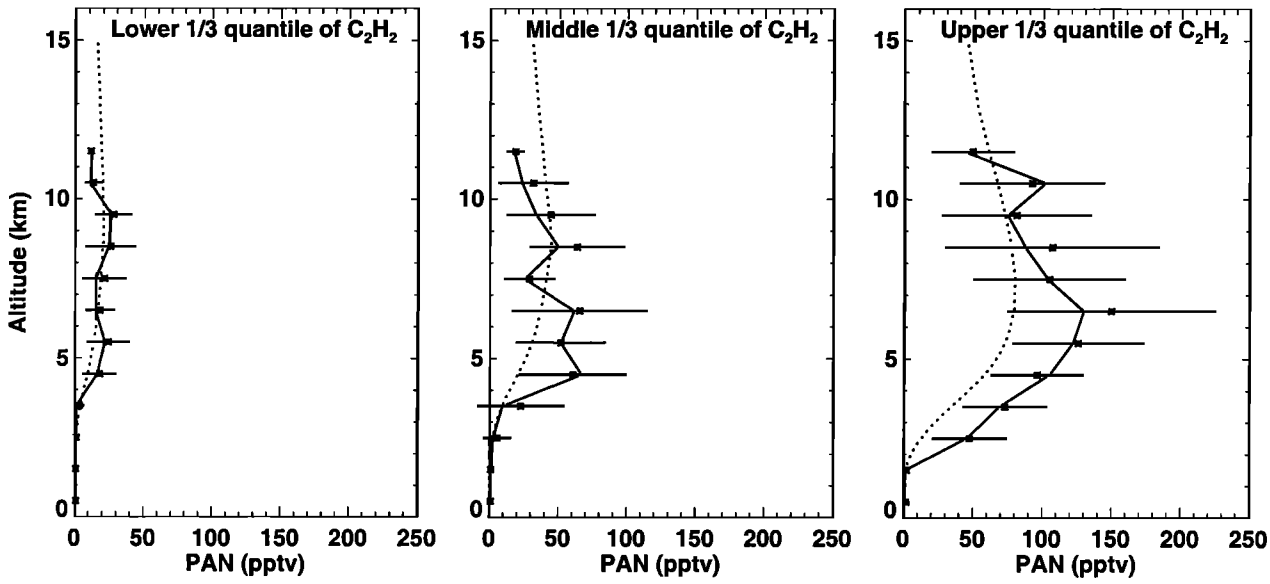

Figure 12. Same as Figure 3 but for peroxyacetylnitrate (PAN). Simulated PAN concentrations are from the standard model.

H_2O_2 by 50-100% is necessary in the model to match observations. Model results indicate that 40-80% of CH_3OOH in the upper troposphere is due to convective transport from the lower troposphere. Photolysis of convected CH_3OOH more than doubles the primary source of HO_x in the region. The reaction of O^1D+H_2O, which is the dominant primary HO_x source in the lower and middle troposphere, is surpassed by photolysis of convected CH_3OOH and photolysis of acetone above 11 km. The latter two sources are also much larger than that from photolysis of convected CH_2O. Convection of CH_3OOH increases the total HO_x source and OH concentration by up to a factor of 3 and 50%, respectively, in the upper troposphere; it increases the production rate of O_3 by about 0.4 ppbv d^{-1} above 11 km. Integrating over the air column of 0-16 km, we find that convection of CH_3OOH has a negligible effect on the column mean OH concentration and increases column O_3 production by only 4%.

In comparison, the effect of biomass burning outflow is much more significant in changing chemistry over the tropical Pacific. We group observations into three equally divided quantiles of C_2H_2 concentrations, because C_2H_2 is a good tracer for biomass burning outflow during PEM-Tropics A. Using the lower one-third quantile of C_2H_2 data as the air masses least influenced by biomass burning outflow, we estimate that 60% (or 9 DU) of O_3 and 75% NO_x enhancements in the air column of 0-12 km are due to import of pollutants from biomass burning regions. The NO_x enhancement increases column O_3 production (0-12 km) by 45%. The import of pollutants increases the column mean OH concentration by a moderate 7% due in part to the offsetting effects of concurrent increases in NO_x and CO concentrations.

The effect of pollutant import into the region is reflected in the budget and concentrations of long-lived chemical species. Whereas short-lived H_2O_2 and CH_3OOH concentrations are generally reproduced based on in situ chemistry and local convective transport within the PEM-Tropics A region, the budget of longer-lived O_3 shows a column O_3 loss a factor of 2 larger than column O_3 production. A model sensitivity study indicates that 50% of O_3 is supplied by lateral import, similar to the finding by *Schultz et al.* [1999]. Peroxyacetylnitrate has a lifetime of about 1 month in the tropical upper troposphere. Model simulations are in much better agreement with PAN observations for the lower one-third quantile of C_2H_2 than those for the middle and upper one-third quantiles of C_2H_2. The underestimate of PAN concentrations for the middle and upper one-third quantiles of C_2H_2 is consistent with pollutant import into the region. Nitric acid also has a long chemical lifetime but is removed efficiently by wet scavenging. As a result, significant direct import of HNO_3 from biomass burning regions is unlikely. Model results are in reasonable agreement with observations for the lower and middle one-third quantiles of C_2H_2. However, the model overestimates HNO_3 concentrations by about a factor of 2 above 4 km for the upper one-third quantile of C_2H_2, as observed previously in other regions of the globe. This discrepancy cannot be explained by recent kinetic data for the reactions of OH with HNO_3 and NO_2 [*Brown et al.*, 1999a, b]. There are two likely explanations: (1) the outflow from biomass burning regions has not reached steady state with respect to HNO_3; and (2) HNO_3 is recycled rapidly back to NO_x by some heterogeneous mechanism in biomass burning outflow.

Acknowledgments. We thank Michael Prather and Martin Schultz for providing useful data. Martin Schultz and anonymous reviewers provided helpful suggestions. We also acknowledge the PEM-Tropics A scientists, DC-8 flight crews, and support staff. In particular, we thank John Bradshaw, Brian Heikes, Glen Sachse, Richard Shetter, Hanwant Singh, and Robert Talbot for their measurements. This work was supported in part by the National Aeronautics and Space Administration (NASA GTE NAG-1-1822).

References

Andreae, M. O., Ocean-atmosphere interactions in the global biogeochemical sulfur cycle, *Mar. Chem., 30,* 1-29, 1990.

Andreae, M. O., E. Atlas, H. Cachier, W. R. Cofer III, G. W. Harris,

G. Helas, R. Koppmann, J.-P. Lacaux, and D. W. Ward, Trace gas and aerosol emissions from savanna fires, in *Biomass Burning and Global Change*, vol. 1, *Remote Sensing, Modeling and Inventory Development, and Biomass Burning in Africa*, edited by J. S. Levine, chap. 27, pp. 278-295, MIT Press, Cambridge, Mass., 1996.

Arnold, F., J. Schneider, K. Gollinger, H. Schlager, P. Schulte, E. Hage, P. D. Whitefield, and P. van Velthoven, Observations of upper tropospheric sulfur dioxide- and acetone-pollution: Potential implications for hydroxyl radical and aerosol formation, *Geophys. Res., Lett., 24,* 57-60, 1997.

Atkinson, R., et al., Evaluated kinetic and photochemical data for atmospheric chemistry, *J. Phys. Chem. Ref. Data, 26*, suppl. VI, 1329-1499, 1997.

Bates, T. S., B. K. Lamb, A. Guenther, J. Dignon, and R. E. Stoiber, Sulfur emissions to the atmosphere from natural sources, *J. Atmos. Chem., 14*, 315-337, 1992.

Blake, N. J., D. R. Blake, B. C. Sive, T.-Y. Chen, F. S. Rowland, J. E. Collins, Jr., G. W. Sachse, and B. E. Anderson, Biomass burning emissions and vertical distribution of atmospheric methyl halides and other reduced carbon gases in the South Atlantic region, *J. Geophys. Res., 101,* 24,151-24,164, 1996.

Blake, N. J., et al., Influence of southern hemispheric biomass burning on midtropospheric distributions of nonmethane hydrocarbons and selected halocarbons over the remote South Pacific, *J. Geophys. Res., 104,* 16,213-16,232, 1999.

Brown, S. S., R. K. Talukdar, and A. R. Ravishankara, Rate constants for the reaction OH + NO_2 + M → HNO_3 + M under atmospheric conditions, *Chem. Phys. Lett., 299,* 277-284, 1999a.

Brown, S. S., R. K. Talukdar, and A. R. Ravishankara, Reconsideration of the rate constant for the reaction of hydroxyl radicals with nitric acid, *J. Phys. Chem., 103,* 3031-3037 , 1999b.

Chatfield, R. B., Anomalous HNO_3 /NO_x ratio of remote tropospheric air: Conversion of nitric acid to formic acid and NO_x ?, *Geophys. Res. Lett., 21*, 2705-2708, 1994.

Chatfield, R. B., and P. J. Crutzen, Sulfur dioxide in remote oceanic air: Cloud transport of reactive precursors, *J. Geophys. Res., 89,* 7111-7132, 1984.

Cohan, D. S., M. G. Schultz, D. J. Jacob, B. G. Heikes, and D. R. Blake, Convective injection and photochemical decay of peroxides in the upper troposphere: Methyl iodide as a tracer of marine convection, *J. Geophys. Res., 104,* 5717-5724, 1999.

Crawford, J., et al., Assessment of upper tropospheric HO_x sources over the tropical Pacific based on NASA GTE/PEM data: Net effect on HO_x and other photochemical parameters, *J. Geophys. Res., 104,* 16,255-16,274, 1999.

Crutzen, P. J., and M. O. Andreae, Biomass burning in the tropics: Impact on atmospheric chemistry and biogeochemical cycles, *Science, 250,* 16,769-16,778, 1990.

Davis, D. D., et al., Assessment of ozone photochemistry in the western North Pacific as inferred from PEM-West A observations during the fall 1991, *J. Geophys. Res., 101,* 2111-2134, 1996a.

Davis, D. D., J. Crawford, S. Liu, S. McKeen, A. Bandy, D. Thornton, and D. Blake, Potential impact of iodine on tropospheric levels of ozone and other critical oxidants, *J. Geophys. Res., 101,* 2135-2147, 1996b.

DeMore, W. B., et al., Chemical kinetics and photochemical data for use in stratospheric modeling, *JPL Publ. 97-4*, 266 pp., 1997.

Dickerson, R. R., et al., Thunderstorms: An important mechanism in the transport of air pollutants, *Science, 35*, 460-465, 1987.

Fan, S.-M., D. J. Jacob, D. L. Mauzerall, J. D. Bradshaw, S. T. Sandholm, D. R. Blake, H. B. Singh, R. W. Talbot, G. L. Gregory, and G. W. Sachse, Origin of tropospheric NO_x over subarctic eastern Canada in summer, *J. Geophys. Res., 99,* 16,867-16,877, 1994.

Fishman, J., C. E. Watson, J. C. Larsen, and J. A. Logan, Distribution of tropospheric ozone determined from satellite data, *J. Geophys. Res., 95,* 3599-3617, 1990.

Fishman, J., J. M. Hoell, R. D. Bendura, R. J. McNeal, and V. W. J. H. Kirchhoff, NSAS GTE TRACE A Experiment (September-October 1992): Overview, *J. Geophys. Res., 101,* 23,865-23,879, 1996.

Gidel, L. T., Cumulus cloud transport of transient tracers, *J. Geophys. Res., 88,* 6587-6599, 1983.

Gierczak, T., J. B. Burkholder, S. Bauerle, and A. R. Ravishankara, Photochemistry of acetone under tropospheric conditions, *Chem. Phys., 231,* 229-244, 1998.

Happell, J. D., and D. W. R. Wallace, Methyl idode in the Greenland/Norwegian Seas and the tropical Atlantic Ocean: Evidence for photochemical production, *Geophys. Res. Lett., 23,* 2105-2108, 1996.

Hauglustaine, D. A., B. A. Ridley, S. Solomon, P. G. Hess, and S. Madronich, HNO_3 /NO_x ratio in the remote troposphere during MLOPEX 2: Evidence for nitric acid reduction on carbonaceous aerosols, *Geophys. Res. Lett., 23,* 2609-2612, 1996.

Hauglustaine, D. A., G. P. Brasseur, S. Walters, P. J. Rasch, J. F. Müller, L. K. Emmons, and M. A. Carroll, MOZART, a global chemical transport model for ozone and related chemical tracers, 2, Model results and evaluation, *J. Geophys. Res., 103,* 28,291-28,335, 1998.

Hoell, J. M., D. D. Davis, D. J. Jacob, M. O. Rodgers, R. E. Newell, H. E. Fuelberg, R. J. McNeal, J. L. Raper, and R. J. Bendura, The Pacific Exploratory Mission in the tropical Pacific: PEM-Tropics A, August-September 1996, *J. Geophys. Res., 104,* 5567-5583, 1999.

Jacob, D. J., et al., Origin of ozone and NO_x in the tropical troposphere: A photochemical analysis of aircraft observations over the South Atlantic basin, *J. Geophys. Res., 101,* 24,235-24,250, 1996.

Jaeglé, L., et al., Observed OH and HO_2 in the upper troposphere suggest a major source from convective injection of peroxides, *Geophys. Res. Lett., 24,* 3181-3184, 1997.

Jaeglé, L., D. J. Jacob, Y. Wang, A. J. Weinheimer, B. A. Ridley, T. L. Campos, G. W. Sachse, and D. E. Hagen, Sources and chemistry of NO_x in the upper troposphere over the United States, *Geophys. Res. Lett., 25,* 1705-1708, 1998.

Kleinman, L. I., Low and high NO_x tropospheric photochemistry, *J. Geophys. Res., 99,* 16,831-16,838, 1994.

Lary, D. J., A. M. Lee, R. Toumi, M. J. Newchurch, M. Pirre, and J. B. Renard, Carbon aerosols and atmospheric photochemistry, *J. Geophys. Res., 102*, 3671-3682, 1997.

Lawrence, M. G., and P. J. Crutzen, The impact of cloud particle gravitational settling on soluble trace gas distributions, *Tellus Ser. B, 50*, 263-289, 1998.

Lind, J. A., and G. L. Kok, Henry's law determinations for aqueous solutions of hydrogen peroxide, methylhydroperoxide, and peroxyacetic acid, *J. Geophys. Res., 91,* 7889-7895, 1986.

Liu, S. C., J. R. McAfee, and R. J. Cicerone, Radon 222 and tropospheric vertical transport, *J. Geophys. Res., 89,* 7291-7297, 1984.

Logan, J. A., M. J. Prather, S. C. Wofsy, and M. B. McElroy, Tropospheric chemistry: A global perspective, *J. Geophys. Res., 86,* 7210-7254, 1981.

McKeen, S. A., et al., Photochemical modeling of hydroxyl and its relationship to other species during the Tropospheric OH Photochemistry Experiment, *J. Geophys. Res., 102,* 6467-6493, 1997a.

McKeen, S. A., T. Gierczak, J. B. Burkholder, P. O. Wennberg, T. F. Hanisco, E. R. Keim, R.-S. Gao, S. C. Liu, A. R. Ravishankara, and D. W. Fahey, The photochemistry of acetone in the upper troposphere: A source of odd-hydrogen radicals, *Geophys. Res. Lett., 24*, 3177-3180, 1997b.

Müller, J.-F., and G. Brasseur, Sources of upper tropospheric HO_x: A three-dimensional study, *J. Geophys. Res., 104,* 1705-1715, 1999.

Olson, J. R., B. A. Baum, D. R. Cahoon, and J. H. Crawford, Frequency and distribution of forest, savanna, and crop fires over tropical regions during PEM-Tropics A, *J. Geophys. Res., 104,* 5865-5876, 1999.

Pickering, K. E., R. R. Dickerson, G. J. Huffman, J. F. Boatman, and A. Schanot, Trace gas transport in the vicinity of frontal convective clouds, *J. Geophys. Res., 93,* 759-773, 1988.

Pickering, K. E., A. M. Thompson, J. R. Scala, W.-K. Tao, R. R. Dickerson, and J. Simpson, Free tropospheric ozone production following entrainment of urban plumes into deep convection, *J. Geophys. Res., 97,* 17,985-18,000, 1992.

Prather, M. J., and D. J. Jacob, A persistent imbalance in HO_x and NO_x photochemistry of the upper troposphere driven by deep tropical convection, *Geophys. Res. Lett., 24,* 3189-3192, 1997.

Rind, D., and J. Lerner, Use of on-line tracers as a diagnostic tool in general circulation model development, 1, Horizontal and vertical transport in the troposphere, *J. Geophys. Res., 101,* 12,667-12,683, 1996.

Schultz, M., et al., On the origin of tropospheric ozone and NO_x over the tropical South Pacific, *J. Geophys. Res., 104,* 5829-5843, 1999.

Schultz, M., D. J. Jacob, J. D. Bradshaw, S. T. Sandholm, J. E. Dibb,

R. W. Talbot, and H. B. Singh, Chemical NO_x budget in the upper troposphere over the tropical South Pacific, *J. Geophys. Res.*, in press, 2000.

Singh, H. B., M. Kanakidou, P. J. Crutzen, and D. J. Jacob, High concentrations and photochemical fate of oxygenated hydrocarbons in the global troposphere, *Nature, 378,* 50-54, 1995.

Smyth, S., et al., Comparison of free troposphere western Pacific air mass classification schemes for the PEM-West A experiment, *J. Geophys. Res., 101,* 1743-1762, 1996.

Talbot, R. W., J. E. Dibb, E. M. Scheuer, D. R. Blake, N. J. Blake, G. L. Gregory, G. W. Sachse, J. B. Bradshaw, S. T. Sandholm, and H. B. Singh, Influence of biomass combustion emissions on the distribution of acidic trace gases over the southern Pacific basin during austral springtime, *J. Geophys. Res., 104,* 5623-5634, 1999.

Talukdar, R. K., J. B. Burkholder, A. M. Schmoltner, J. M. Roberts, R. R. Wilson, and A. R. Ravishankara, Investigation of the loss processes for peroxyacetyl nitrate in the atmosphere: UV photolysis and reaction with OH, *J. Geophys. Res., 100,* 14,163-14,173, 1995.

Trainer, M., E. Y. Hsie, S. A. McKeen, T. Tallamraju, D. D. Parish, F. C. Fehsenfeld, and S. C. Liu, Impact of natural hydrocarbons on hydroxyl and peroxy radicals at a remote site, *J. Geophys. Res., 92,* 11,879-11,894, 1987.

Trainer, M., et al., Observations and modeling of the reactive nitrogen photochemistry at a rural site, *J. Geophys. Res., 96,* 3045-3063, 1991.

Wang, Y., D. J. Jacob, and J. A. Logan, Global simulation of tropospheric O_3-NO_x-hydrocarbon chemistry, 1, Model formulation, *J. Geophys. Res., 103,* 10,713-10,725, 1998a.

Wang, Y., J. A. Logan, and D. J. Jacob, Global simulation of tropospheric O_3-NO_x-hydrocarbon chemistry, 2, Model evaluation and global ozone budget, *J. Geophys. Res., 103,* 10,727-10,755, 1998b.

Wennberg, P. O., et al., Hydrogen radicals, nitrogen radicals, and the production of ozone in the middle and upper troposphere, *Science, 279,* 49-53, 1998.

D. R. Blake and T.-Y. Chen, Department of Chemistry, University of California, Irvine, CA 92697-2025.

S. C. Liu, S. T. Sandholm, and H. Yu, School of Earth and Atmospheric Sciences, Georgia Institute of Technology, Atlanta, GA 30332-0340.

Y. Wang, Department of Environmental Sciences, Rutgers University, 14 College Farm Road, New Brunswick, NJ 08901-8551. (yhw@envsci.rutgers.edu)

(Received July 6, 1999; revised October 5, 1999;
accepted November 11, 1999.)